Citation: CPT Pharmacometrics Syst. Pharmacol. (2016) 5, 565–574; doi:10.1002/psp4.12126

ORIGINAL ARTICLE

Assessing the Impact of Tissue Target Concentration Data on Uncertainty in *In Vivo* Target Coverage Predictions

A Tiwari[1], H Luo[2], X Chen[1], P Singh[1], I Bhattacharya[3], P Jasper[2], JE Tolsma[2], HM Jones[1], A Zutshi[4] and AK Abraham[5]

Understanding pharmacological target coverage is fundamental in drug discovery and development as it helps establish a sequence of research activities, from laboratory objectives to clinical doses. To this end, we evaluated the impact of tissue target concentration data on the level of confidence in tissue coverage predictions using a site of action (SoA) model for antibodies. By fitting the model to increasing amounts of synthetic tissue data and comparing the uncertainty in SoA coverage predictions, we confirmed that, in general, uncertainty decreases with longitudinal tissue data. Furthermore, a global sensitivity analysis showed that coverage is sensitive to experimentally identifiable parameters, such as baseline target concentration in plasma and target turnover half-life and fixing them reduces uncertainty in coverage predictions. Overall, our computational analysis indicates that measurement of baseline tissue target concentration reduces the uncertainty in coverage predictions and identifies target-related parameters that greatly impact the confidence in coverage predictions.
CPT Pharmacometrics Syst. Pharmacol. (2016) **5**, 565–574; doi:10.1002/psp4.12126; published online 22 October 2016.

Study Highlights

WHAT IS THE CURRENT KNOWLEDGE ON THE TOPIC?

☑ Minimal PK/PD models have been used to study and predict the distribution of mAbs and their coverage of target in various tissues. The utility of these models depend on our understanding of the minimal data requirements for such models and the key parameters that significantly influence predictions. It is currently not known how tissue data or its lack thereof and which model parameters impact target coverage predictions.

WHAT QUESTION DID THIS STUDY ADDRESS?

☑ This study evaluates the impact of (i) increasing quantities of tissue target concentration data and (ii) information about model parameters on uncertainty in tissue target coverage predictions of a minimal PK/PD model.

WHAT THIS STUDY ADDS TO OUR KNOWLEDGE

☑ This study shows that measurement of baseline target concentration in tissue substantially reduces the uncertainty in target coverage predictions. Additionally, it identifies key model parameters that greatly impact the confidence in coverage predictions.

HOW THIS MIGHT CHANGE DRUG DISCOVERY, DEVELOPMENT, AND/OR THERAPEUTICS

☑ Understanding the determinants of uncertainty in target coverage predictions and the basic data requirements of minimal PK/PD models enhances their utility in ensuring the mechanism has been tested at adequate target engagement and guiding subsequent decision-making with regard to dose selection in early clinical trials.

Protein-based therapeutics, such as monoclonal antibodies (mAbs), bispecific antibodies, Fc-fusion proteins, hormones, cytokines, and antibody-drug conjugates are increasingly being developed to treat a variety of diseases.[1,2] This interest is mainly due to their high target specificity and longer half-lives compared to small molecule drugs. The distribution of mAb-based therapeutics into tissues is limited because of their large size,[3,4] but is nevertheless crucial for understanding the ability of the drug to effectively engage the target in diseased tissues. In drug discovery, mathematical models are often used to select compounds and identify safe and efficacious doses, thereby offering a quantitative approach to improve drug development and decision-making.[5] Several models describing standard target-mediated drug disposition[6–9] to more complex physiologically-based pharmacokinetics (PK)[10–12] incorporate distribution of protein-based therapeutics into peripheral tissues. These models have been used extensively to predict tissue PK and in some cases pharmacodynamics (PD) and efficacy. Recently, minimal models of drug binding and distribution[13–16] have gained popularity. Minimal models are amenable to characterizing PK/PD relationships in specific tissues, like the gastrointestinal tract in Crohn's disease and synovium in rheumatoid arthritis (RA). These disorders are marked by tissue overexpression of cytokines, like tumor necrosis factor α (TNFα) and mAb therapies neutralizing TNFα have been shown to be effective.[17,18] Here after, we refer to these minimal models characterizing specific tissues as site of action (SoA) models.

[1]Department of Pharmacokinetics, Dynamics, and Metabolism, Pfizer Worldwide R&D, Cambridge, Massachusetts, USA; [2]RES Group, Needham, Massachusetts, USA; [3]Quantitative Clinical Sciences, PharmaTherapeutics R&D, Pfizer Inc., Cambridge, Massachusetts, USA; [4]Current address: EMD Serono, Billerica, Massachusetts, USA; [5]Current address: Pharmacokinetics, Pharmacodynamics & Drug Metabolism, Merck Research Laboratories, West Point, PA, USA. *Correspondence: A Tiwari (abhinav.tiwari@pfizer.com)
Received 28 July 2016; accepted 19 August 2016; published online on 22 October 2016. doi:10.1002/psp4.12126

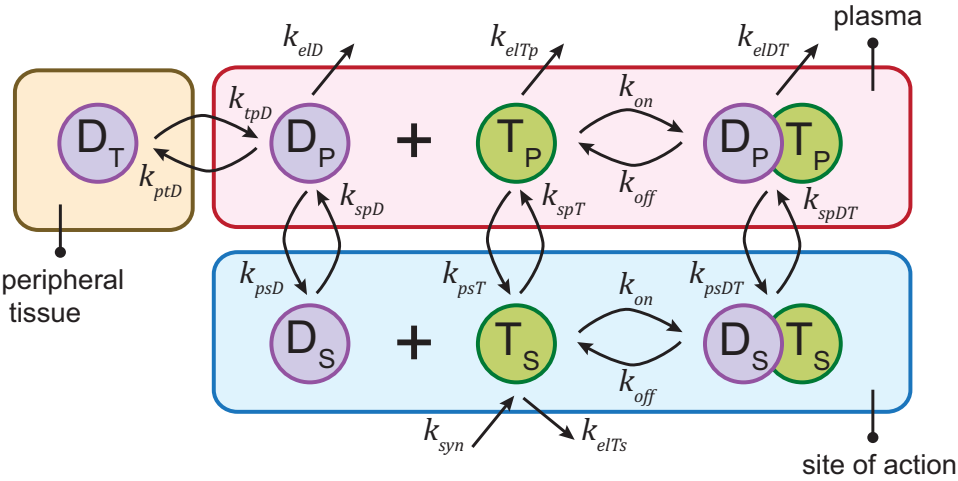

Figure 1 Site of action (SoA) model. Drug is administered intravenously and then distributes into the tissue of interest (SoA) and peripheral tissue. In the central and site of action compartments, drug binds reversibly to target protein to form drug-target complex. Both the target and complex can distribute between these two compartments. Target protein is synthesized only in the SoA compartment but gets eliminated in both compartments. Drug and complex are eliminated only in the central compartment.

Pharmacological target coverage, defined here as the percentage of target bound by drug, is fundamental to drug discovery and development. The lack of understanding of coverage and/or its relationship to safety and efficacy could increase the risk of failure for a promising molecule. The SoA models (**Figure 1**) have been used to study and predict mAb distribution and target coverage in various tissues.[11,13,14,19] For example, an SoA model examined interactions between adalimumab and TNFα in central, peripheral, and synovium compartments and compared the efficacy of intra-articular vs. systemic administration of adalimumab for treatment of RA.[19] In another example, an SoA model for anti-interleukin (IL)-1β mAb ACZ885 was used to characterize total target concentrations in plasma and predict target-engagement in peripheral tissues.[13] Another model examined the efficacy of bispecific antibodies against soluble and membrane-bound targets for treatment of systemic lupus erythematosus and against two other soluble targets in ulcerative colitis and asthma.[14] Lastly, an SoA model integrated antibody PK and total CXCL13 levels in mouse serum and spleen to predict target coverage, which was in turn linked to germinal center response.[20] The above examples highlight the utility of SoA models in predicting target coverage (using free target suppression profiles), which is increasingly being used to select doses for clinical trials. Understanding coverage becomes particularly important in cases where a sensitive biomarker is unavailable to understand downstream pharmacology. Additionally, target coverage enables design of preclinical toxicology studies, calculations of safety margins, and ultimately design of clinical studies.

The importance of SoA models to predict tissue target coverage depends on our understanding of the minimal data requirements for such models and key parameters that significantly influence predictions. Currently, it is not known how tissue data or its lack thereof impacts coverage predictions. Typically, tissue data represent measurements using a total target assay that measures free target at baseline (pre-dose sample) and total target (free + drug-bound) after drug administration. The objective of this study is to evaluate the impact of increasing quantities of longitudinal tissue target concentration data on uncertainty in target coverage predictions.

METHODS

Mathematical model

An ordinary differential equation-based model with plasma, SoA, and peripheral tissue compartments was developed for this analysis (**Figure 1**). Below is the system of ordinary differential equations:

$$\frac{dD_P}{dt} = k_{spD} D_S \frac{V_S}{V_P} + k_{tpD} D_T \frac{V_T}{V_P} - k_{psD} D_P - k_{ptD} D_P + k_{off} DT_P - k_{on} D_P T_P - k_{elD} D_P$$

$$\frac{dD_S}{dt} = k_{psD} D_P \frac{V_P}{V_S} - k_{spD} D_S + k_{off} DT_S - k_{on} D_S T_S$$

$$\frac{dD_T}{dt} = k_{ptD} D_P \frac{V_P}{V_T} - k_{tpD} D_T$$

$$\frac{dDT_P}{dt} = k_{spDT} DT_S \frac{V_S}{V_P} - k_{psDT} DT_P + k_{on} D_P T_P - k_{off} DT_P - k_{elDT} DT_P$$

$$\frac{dDT_S}{dt} = k_{psDT} DT_P \frac{V_P}{V_S} - k_{spDT} DT_S + k_{on} D_S T_S - k_{off} DT_S$$

$$\frac{dT_P}{dt} = k_{spT} T_S \frac{V_S}{V_P} - k_{psT} T_P + k_{off} DT_P - k_{on} D_P T_P - k_{elTp} T_P$$

$$\frac{dT_S}{dt} = k_{psT} T_P \frac{V_P}{V_S} - k_{spT} T_S + k_{off} DT_S - k_{on} D_S T_S + \frac{k_{syn}}{V_S} - k_{elTs} T_S$$

where D_i, DT_i, and T_i represent concentrations of free drug, drug-target complex, and free target in plasma $(i=P)$ or SoA $(i=S)$ compartment, respectively. D_T is free drug

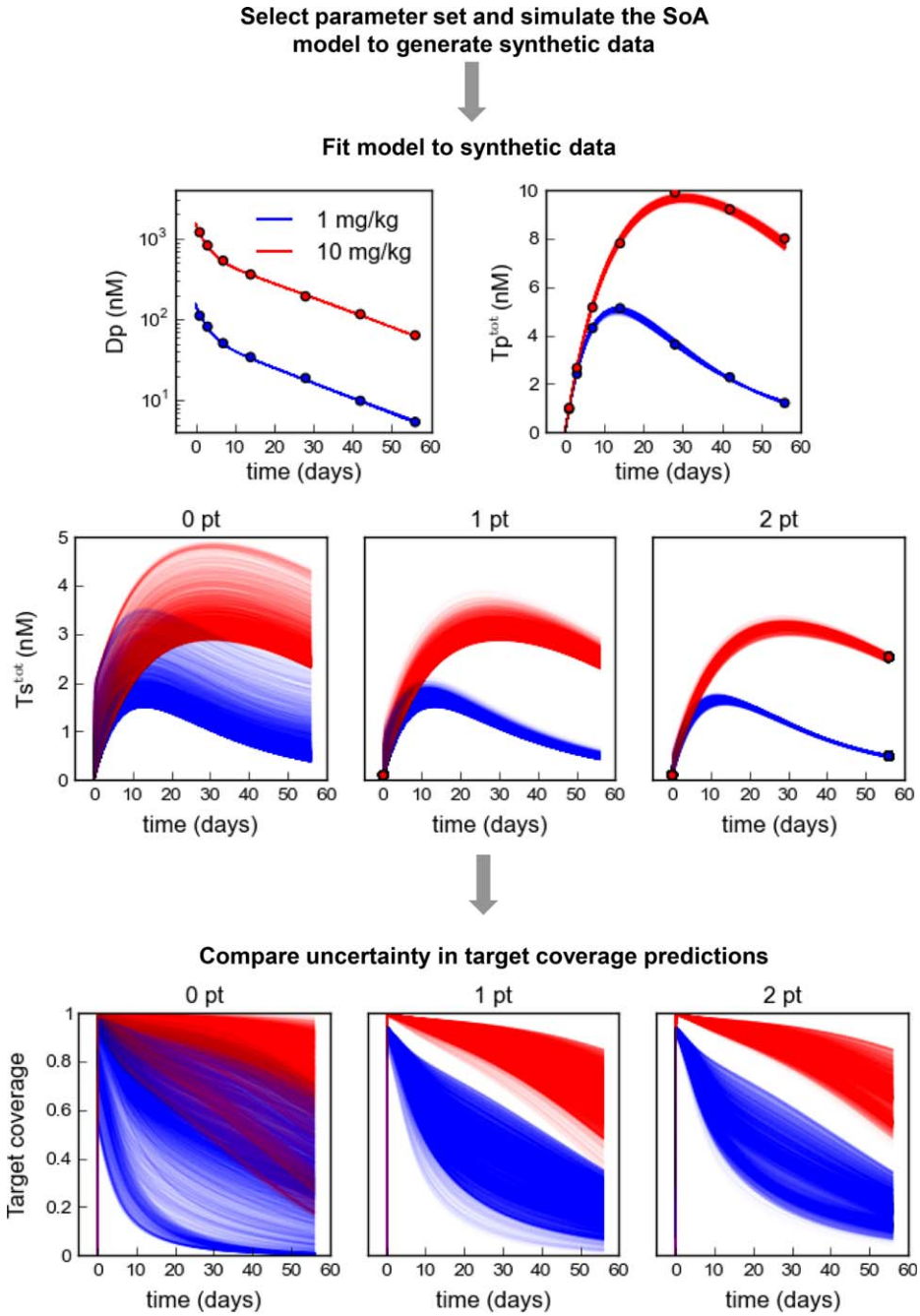

Figure 2 Flow chart of coverage uncertainty analysis. First, a parameter set selected from **Table 1** together with fixed values of remaining model parameters is used to simulate the site of action (SoA) model for 1 mg/kg (blue) and 10 mg/kg (red) i.v. dosing of drug to generate synthetic data: D_P, T_P^{tot}, and T_S^{tot} time profiles (blue and red circles). Next, the SoA model is fit at least 3,000 times (blue and red curves) to synthetic data for three different cases: 0, 1, or 2 T_S^{tot} data points. Each curve in these panels represents an independent model fit. Finally, the uncertainty in target coverage predictions at a given time is quantified as SD of all the predicted values. Each curve in target coverage panels represents a model prediction corresponding to one of the model fits.

concentration in the peripheral tissue compartment. Initial conditions for ordinary differential equations are: $D_P(0) = (Dose * BWT * 10^6)/(MWT * V_P)$, $T_P(0) = T_{P0}$, $T_S(0) = T_{S0}$, and $D_T(0) = D_S(0) = DT_P(0) = DT_S(0) = 0$. $BW = 70$ kg is typical body weight of human, $MWT = 150,000$ daltons is drug (mAb) molecular weight, and V_P is plasma compartment volume in liters.

Intravenous (i.v.) administration of a drug is modeled as a bolus into a plasma compartment. A drug not bound to target distributes into peripheral (V_T) and SoA (V_S) compartments. For this analysis, gut tissue was selected as an example of SoA. Drug reversibly binds the target to form a drug-target complex. Binding kinetics is characterized by second-order association (k_{on}) and first-order dissociation

(k_{off}) rate constants. The k_{on} was fixed to a diffusion-limited maximum value[21] and $k_{off} = k_{on} K_D$, in which K_D is the equilibrium dissociation constant for drug-target binding. Note that we performed all our analysis with respect to K_D instead of k_{off}, as it is relatively easier to determine experimentally and available more widely.

This version of an SoA model assumes the drug, target, and complex can distribute between plasma and SoA compartments, which is only valid for soluble targets as their distribution is primarily governed by diffusion. In many cases, we lack information regarding distribution rates, particularly for target. In such cases, a reduced model that ignores such processes may be used.[20] To emulate a disease state, it is assumed that free target is primarily synthesized in SoA (typically overexpressed), but is degraded both in plasma and SoA. Drug and complex are assumed to be eliminated systemically from the plasma compartment. Model parameters are listed in **Supplementary Tables S1 and S2**.

Figure 2 describes various steps in the analysis. Step 1: select parameter set and simulate SoA model to generate synthetic data. Step 2: fit model to synthetic data (drug PK, plasma target kinetics, and three different quantities of tissue target data). Step 3: compare uncertainty in target coverage predictions across three cases. Details of each step are discussed below.

Step 1: Select parameter set and simulate model to generate synthetic data

Five SoA model parameters, K_D, baseline target concentration in plasma (T_{P0}), ratio of baseline target concentrations in SoA to plasma ($Ratio_T$), target half-life in plasma (*thalfTp*), and target half-life in SoA (*thalfTs*), were set to a low/high value to obtain 32 (2^5) partial parameter sets that satisfy three different criteria: $T_{P0} < K_D \leq T_{S0}$, $K_D < T_{P0} < T_{S0}$, and $T_{P0} < T_{S0} < K_D$ (**Table 1**). Low and high values for each parameter were selected to represent physiologically relevant bounds. Each of these partial parameter sets was combined with fixed values for the remaining model parameters (**Supplementary Tables S1 and S2**) to obtain complete parameter sets. These fixed values describe the typical PK of an mAb[22,23] and the distribution of mAbs and target between plasma and SoA. The model was then simulated using these complete parameter sets for 1 and 10 mg/kg single i.v. doses to generate synthetic data: concentration-time profiles of D_P, total target concentration in plasma (T_P^{tot}) and SoA (T_S^{tot}), up to 56 days. We considered 16 data points in plasma, 8 each for D_P and T_P^{tot} at days 0, 1, 3, 7, 14, 28, 42, and 56. The sampling schedule was based on a typical internal clinical trial design. We considered three different cases of tissue data (T_S^{tot}) – 0, 1, or 2 data points per dose. The first case is self-explanatory, whereas the second and third cases correspond to baseline target measurement (day 0) only, and baseline and end-of-treatment (day 56) total target measurements, respectively. We assumed lack of access to tissue-level data during treatment. In addition, to account for experimental variability, a maximum of 5% noise (random variability) was added to each synthetic data point.

Step 2: Fit model to synthetic data

The control parameterization method[24] implemented in J2 Dynamic Modeling and Optimization Software (RES Group, 2016) was used to minimize the following objective function for $\vec{p} = \{CL_{Dt},\ CL_{Ds}, CL_{Ts}, K_D,\ T_{P0}, Ratio_T,\ thalfTp,\ thalfTs\}$:

$$O(\vec{p}) = \sqrt{\sum_t \left(\ln(D_P) - \ln\left(D_P^{data}\right)\right)^2 + \sum_t \left(\ln\left(T_P^{tot}\right) - \ln\left(T_P^{tot,data}\right)\right)^2 + \sum_t \left(\ln\left(T_S^{tot}\right) - \ln\left(T_S^{tot,data}\right)\right)^2}$$

where t represents time points.

The model was fit to each synthetic dataset 10,000 times and only those fits were accepted, which resulted in <7% error for each fitted data point. For each of the 10,000 optimizations, initial guesses for model parameters were randomly generated using a uniform and independent sampling (in logarithmic space) within bounds listed in **Supplementary Table S3**.

Step 3: Uncertainty in target coverage predictions

Target coverage at SoA was calculated as follows:

$$coverage = 1 - \frac{T_S}{T_{S0}}$$

where T_{S0} and T_S are baseline and free target concentration in SoA. Note $T_{S0} = T_S^{tot}(t=0)$. Uncertainty in coverage predictions at a given time is quantified as its SD for all accepted fits. Uncertainty analysis was performed twice, first when all parameters in $\vec{p}$ were estimated and second when a sensitive parameter (T_{P0} or *thalfTp*) was fixed and the remaining parameters were estimated.

RESULTS

Uncertainty in target coverage predictions decreases with additional tissue data

We systematically investigated the impact of increasing amounts of tissue data on uncertainty in target coverage predictions in SoA. Hereafter, coverage predictions always refer to predictions in the SoA compartment. We sampled 32 different parameter sets (**Table 1**, see Methods) based on physiologically relevant upper/lower bounds for five target-related parameters – K_D, T_{P0}, $Ratio_T$, *thalfTp*, and *thalfTs*. These parameter sets were used to generate synthetic data (for 1 and 10 mg/kg i.v. doses) that included concentration-time profiles for the drug, total target in plasma, and total target in SoA. Subsequently, we fit the model

Table 1 Partial parameter sets used to generate the synthetic data

Case	K_D (nM)	T_{P0} (nM)	$Ratio_T$ (-)	*thalfTp* (h)	*thalfTs* (h)
1	0.1	0.02	5	0.5	0.5
2	0.1	0.02	5	0.5	24
3	0.1	0.02	5	24	0.5
4	0.1	0.02	5	24	24
5	0.1	0.02	100	0.5	0.5
6	0.1	0.02	100	0.5	24
7	0.1	0.02	100	24	0.5
8	0.1	0.02	100	24	24
9	10	0.2	100	0.5	0.5
10	10	0.2	100	0.5	24
11	10	0.2	100	24	0.5
12	10	0.2	100	24	24
13	0.1	0.2	5	0.5	0.5
14	0.1	0.2	5	0.5	24
15	0.1	0.2	5	24	0.5
16	0.1	0.2	5	24	24
17	0.1	0.2	100	0.5	0.5
18	0.1	0.2	100	0.5	24
19	0.1	0.2	100	24	0.5
20	0.1	0.2	100	24	24
21	10	0.02	5	0.5	0.5
22	10	0.02	5	0.5	24
23	10	0.02	5	24	0.5
24	10	0.02	5	24	24
25	10	0.02	100	0.5	0.5
26	10	0.02	100	0.5	24
27	10	0.02	100	24	0.5
28	10	0.02	100	24	24
29	10	0.2	5	0.5	0.5
30	10	0.2	5	0.5	24
31	10	0.2	5	24	0.5
32	10	0.2	5	24	24

Each of the five parameters – K_D, T_{P0}, $Ratio_T$, *thalfTp*, and *thalfTs* – was set to a low or a high value to arrive at 32 (2^5) partial parameter sets, which lie in three different regimes: $T_{P0} < K_D \leq T_{S0}$ (orange), $K_D < T_{P0} < T_{S0}$ (yellow), and $T_{P0} < T_{S0} < K_D$ (green). All these were then combined with the fixed values for the remaining parameters to obtain complete parameter sets that were used to generate synthetic data.

to the synthetic data and calculated uncertainty in target coverage predictions at end-of-treatment.

Results from this analysis are presented in **Table 2**, in which rows represent parameter sets 1 to 32 and columns represent the number of tissue data points (0, 1, or 2). In the majority of cases that were analyzed, uncertainty in target coverage predictions decreased with additional tissue data (compare the numbers along a row in **Table 2**) for both 1 and 10 mg/kg i.v. doses. This trend of reduction in uncertainty with additional tissue data also holds true for multiple doses (**Supplementary Figure S1**), treatment duration of 28 days (**Supplementary Table S4**), and higher maximum noise (20%) in synthetic data (**Supplementary Table S5**), although the degree of uncertainty is different. Uncertainty in coverage predictions dropped substantially with inclusion of one tissue data point. Results for 1 and 10 mg/kg contain 5 and 14 cases, respectively, in which color changes (compare across a row in **Table 2**) between the first and second columns, signifying a reduction in uncertainty. However, if the number of tissue data points in these cases is increased to two, then <30% of these cases (1/5 for 1 mg/kg and 4/14 for 10 mg/kg) show a substantial reduction in uncertainty in coverage predictions.

Results for 1 and 10 mg/kg also contain 27 and 18 cases, respectively, in which the color does not change between the first and second columns, implying a marginal or no reduction in coverage uncertainty. Finally, if the number of tissue data points for the remaining cases (after removing the ones with intrinsically low or high uncertainty) is increased from one to two, then coverage uncertainty drops considerably (i.e., color change) for all of them. In all cases except one, inclusion of two tissue data points resulted in <10% uncertainty.

Table 2 Uncertainty in target coverage predictions decreases with additional tissue data

	1 mg/kg			10 mg/kg		
Case	0 pt	1 pt	2 pt	0 pt	1 pt	2 pt
1	0.19	0.07	0.07	0.2	0.1	0.09
2	0.19	0.16	0.11	0.22	0.15	0.09
3	0.22	0.11	0.07	0.12	0.03	0.02
4	0.05	0.02	0.02	0.01	0	0
5	0.02	0.02	0.01	0.08	0.05	0.07
6	0.23	0.13	0.02	0.11	0.03	0.01
7	0.03	0.03	0.01	0.05	0.05	0.02
8	0.08	0.02	0.02	0.01	0	0
9	0	0	0	0.03	0.01	0.01
10	0.31	0.3	0.01	0.3	0.08	0.01
11	0	0	0	0.02	0.02	0.01
12	0.12	0.09	0	0.04	0.02	0
13	0.05	0.02	0.01	0.19	0.1	0.05
14	0.09	0.04	0.01	0.25	0.04	0.04
15	0.01	0.02	0.01	0.01	0.01	0.01
16	0.05	0.02	0.02	0	0	0
17	0	0	0	0.01	0	0
18	0.18	0.19	0.01	0.03	0.01	0
19	0	0	0	0	0	0
20	0.08	0.07	0.01	0	0	0
21	0.02	0.02	0	0.11	0.07	0.01
22	0.07	0.05	0	0.23	0.14	0.01
23	0.03	0.01	0.01	0.06	0.02	0.02
24	0.29	0.18	0.01	0.2	0.06	0.02
25	0.01	0.01	0	0.07	0.05	0.01
26	0.28	0.31	0.01	0.2	0.12	0
27	0.01	0.01	0.01	0.03	0.02	0.02
28	0.28	0.15	0	0.19	0.04	0
29	0.01	0.01	0	0.06	0.04	0
30	0.3	0.15	0	0.33	0.17	0.01
31	0.01	0.01	0.01	0.02	0.01	0.01
32	0.31	0.14	0	0.21	0.05	0.01

Heat maps depict the uncertainty in target coverage for 1 mg/kg (left) and 10 mg/kg (right) i.v. doses at the end-of-treatment (56 days). Colors red, yellow, and green represent uncertainty >0.1, between 0.05 and 0.1, and <0.05, respectively. Each heat map shows uncertainty for 32 different cases (listed in **Table 1**) with 0, 1, and 2 tissue data points (left, middle, and right columns, respectively).

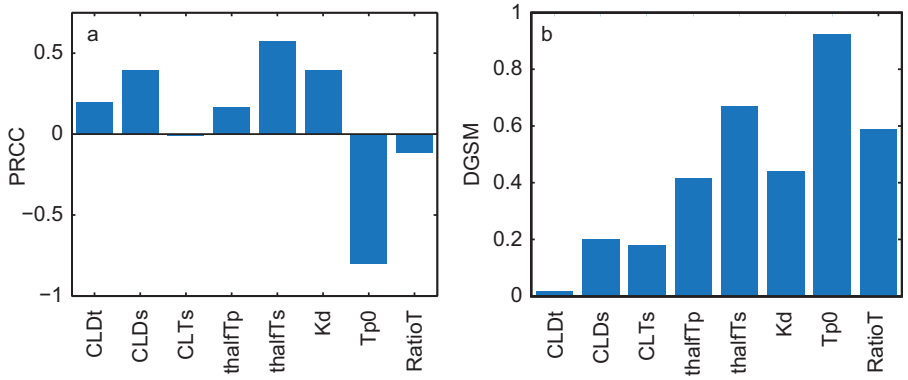

Figure 3 Global sensitivity analysis identifies parameters that affect target coverage. (**a**) Partial rank correlation coefficients (PRCCs) and (**b**) derivative-based global sensitivity measure (DGSM) quantify the sensitivity of coverage to various model parameters at 56 days after a 1 mg/kg i.v. treatment. A PRCC greater (less) than 0 signifies that target coverage increases (decreases) with increase in the parameter.

Target coverage is most sensitive to T_{P0} and $thalf_{Ts}$

Next, we used two different global sensitivity analysis (GSA) methods (see **Supplementary Material** for details), the partial rank correlation coefficients[25] (PRCCs) and the derivative-based global sensitivity measure,[26] to examine the sensitivity of target coverage to various model parameters (**Figure 3 and Supplementary Figure S1**). Both methods showed coverage is most sensitive to T_{P0} and *thalfTs*, and relatively less sensitive to K_D. On the other hand, coverage was least sensitive to the distribution clearance of the drug between plasma and peripheral compartments (CL_{Dt}) and the distribution clearance of the target between plasma and SoA compartment (CL_{Ts}), irrespective of the method used. Likewise, the distribution clearance (CL_{Ds}) of the drug between plasma and SoA compartment was found to have minimal impact on coverage by the derivative-based global sensitivity measure method. However, the PRCC method scored it as a moderately sensitive parameter. For the remaining two parameters, $Ratio_T$ and *thalfTp*, the impact was classified as low to moderate depending on the method used. PRCC classified these two as having a small impact on coverage, whereas derivative-based global sensitivity measure categorized them as having moderate impact. Overall, sensitivity analysis provided a global understanding of the sensitivity of target coverage to various parameters.

Fixing sensitive parameters further reduces uncertainty in target coverage predictions

GSA showed target coverage is most sensitive to T_{P0} and *thalfTs*, thereby suggesting that including information about either of these parameters in the model will reduce uncertainty in coverage predictions. Generally, prior knowledge of *in vivo thalfTs* is either nonexistent or challenging to obtain through experiments. On the other hand, it is relatively easy to measure baseline target concentration in plasma (i.e., T_{P0}). Therefore, we fixed T_{P0} and repeated the uncertainty analysis for all single-tissue data point (middle column) cases in **Table 2** with >5% uncertainty (orange and red cases) in coverage predictions at 1 mg/kg. We found fixing T_{P0} reduced uncertainty in coverage predictions for 6 of 13 cases, albeit by only a small amount, as evident from the color gradient (**Table 3**, third column). We also repeated our uncertainty analysis after fixing *thalfTp*. Fixing *thalfTp* reduces uncertainty in coverage predictions (more than after fixing T_{p0}), especially in cases that represent an optimized mAb ($T_{P0} < K_D \leq T_{S0}$ and $K_D < T_{P0} < T_{S0}$, case numbers $\leq$24; **Table 3**, second column). This trend of reduction in uncertainty after fixing T_{P0} and *thalfTp* also holds true for treatment duration of 28 days (**Supplementary Table S6**). Finally, although GSA showed K_D to be moderately sensitive, we did not perform a comprehensive analysis after fixing it, as initial estimates are often based on *in vitro* methods that depend on measurement technique and may not be consistent with the *in vivo* estimate. Instead, we selected case 1 as an example to demonstrate the impact of fixing K_D. **Figure 4a** shows fixing K_D substantially reduces uncertainty in coverage predictions when the baseline target concentration in tissue is known. Notably, this reduction in uncertainty was greater than that achieved after fixing $Ratio_T$, *thalfTp*, and T_{P0} (**Figure 4b–d**), thereby underscoring the importance of obtaining an accurate K_D measurement. For all these parameters, inclusion of a second tissue data point at end-of-treatment contributed marginally to reduction in uncertainty (**Figure 4**, third column).

DISCUSSION

Quantitative understanding of clinical endpoints and their relationship to target coverage is fundamental to drug development. For therapeutic areas, such as oncology or immune-mediated disorders in which coverage requirements are generally unknown, dose selection and escalation are primarily driven by safety (i.e., maximum tolerated dose). Under this empirical paradigm, doses required for efficacy may not be tested adequately and may be either too low or too high. Furthermore, relationships among exposure, coverage, efficacy, and safety signals may be unknown, which could lead to suboptimal use of patients and resources. To address these inefficiencies in the absence of a biomarker, predicted tissue coverage could be

Table 3 Fixing model parameters further reduces uncertainty in target coverage predictions

	1 mg/kg			10 mg/kg		
Case	1 pt	1 pt, thalfTp	1 pt, Tp0	1 pt	1 pt, thalfTp	1 pt, Tp0
1	0.07	0.03	0.07	0.1	0.02	0.1
2	0.16	0.03	0.09	0.15	0.01	0.08
3	0.11	0.01	0.06	0.03	0	0.02
6	0.13	0.02	0.06	0.03	0	0.02
10	0.3	0.22	0.05	0.08	0.05	0.05
12	0.09	0.01	0.07	0.02	0	0.01
18	0.19	0.16	0.17	0.01	0.02	0.02
20	0.07	0.04	0.07	0	0	0
24	0.18	0.2	0.08	0.06	0.06	0.02
26	0.31	0.23	0.23	0.12	0.06	0.09
28	0.15	0.02	0.07	0.04	0	0.02
30	0.15	0.16	0.14	0.17	0.19	0.23
32	0.14	0.11	0.16	0.05	0.03	0.06

Heat maps depict the uncertainty in target coverage for selected cases before (left column) and after fixing *thalfTp* (middle column) and T_{P0} (right column). Selected cases are the ones that had >5% uncertainty in target coverage with 1 tissue data point (baseline target concentration) for 1 mg/kg i.v. treatment in **Table 2**. Colors have the same meaning as in **Table 2**.

used to provide confidence that the mechanism has been tested. A key challenge is whether one can trust tissue-level predictions, when target levels have been measured only in plasma and relevant tissue data is unavailable. To alleviate this risk, we adopted a computational approach to understand uncertainty in coverage predictions for any soluble target and this can be easily extended to include membrane-bound targets. Of late, physiologically-based SoA models are increasingly being used to characterize PK/PD data.[10–12] However, to the best of our knowledge, a detailed analysis of data requirements for such models is lacking. These models are reasonably complex with numerous parameters, and, therefore, fitting them to limited data could result in significant parameter uncertainty.[27] This uncertainty may undermine model predictions related to target coverage and subsequent dose selection. Suboptimal doses significantly contribute toward cost-of-failure by increasing development and opportunity costs. Assuming the proposed SoA model reasonably characterizes underlying dynamics, our analysis identifies important model features and minimal data requirements to increase confidence in model predictions.

Our analysis focused on mAbs, which, unlike lipophilic small molecules, do not distribute extensively and rapidly within tissues and are primarily limited to interstitial spaces. Generally, clinically viable doses for mAbs range from 0.1 to 10 mg/kg.[28] Irrespective of the absolute dose levels used here, the key goal was to ensure a sufficient range of mAb concentrations relative to target, and thereby a range of target coverage. In tissue interstitium, mAb concentration was constrained to be lower than plasma, an assumption recently validated by experiments that measured plasma and dermal interstitial concentration of IL-17 and anti-IL-17 mAb (secukinumab) in healthy volunteers and patients with moderate to severe psoriasis.[3] The mAb concentrations observed in dermal interstitial perfusate of healthy volunteers and patients with psoriasis were 23% and 35% of plasma levels, respectively. The interstitium of most tissues, except skin, which are important from a disease perspective, may not have a distribution volume large enough to impart the biphasic PK characteristic of mAbs.[23] Hence, a tissue compartment signifying "rest of body" was included to impart biphasic PK. This "rest of body" nonspecific interstitium tissue volume equals peripheral volume (3.1 L) reported for mAbs.[23] In many inflammatory disorders, only certain tissues are affected (e.g., synovial joints in RA, gut in Crohn's disease, and skin in psoriasis). This does not prevent distribution of soluble targets to other tissues; however, their impact on disease effects or target kinetics at SoA may be negligible. From a model parsimony standpoint, selecting a tissue that is most relevant as the SoA seems appropriate. Alternatively, for diseases such as lupus, multiple organ involvement may need to be considered, and, in such a scenario, a lumped tissue interstitial volume could represent SoA. In various diseases, select cytokines are elevated in specific tissues and their high local concentrations are generally thought to be responsible for the underlying inflammation. For example, high concentrations of TNFα, IL-1β, IL-8, and IL-6 have been reported in the synovial fluid of RA and psoriatic arthritis patients.[29,30] Another study reported TNFα, TNFβ, interferon-α, interferon-γ, and IL-8 levels in psoriatic lesional samples were >10 times higher than normal heel skin.[31] High TNFα concentrations have also been measured in patients with inflammatory bowel disease.[32] To maintain mass balance, the model assumes that cytokine degradation occurs either locally through specific target interactions or systemically through nonspecific clearance mechanisms in blood.[33]

Some model assumptions have been discussed above, like target and complex, do not distribute to any tissue except SoA; target is only synthesized in SoA; drug does not impact target synthesis; and drug and complex are not eliminated in SoA. These assumptions can be modified based on the mechanism of action of the drug and/or additional knowledge about the target. For example, the existing model can be modified to include additional mechanisms, like target synthesis in blood and other diseased tissues. However, unless data are available to inform fractional target synthesis in each compartment, such a model may quickly run into parameter identifiability issues. Fraction of target synthesis occurring in blood vis-à-vis SoA will also affect target flux between these compartments. Further, if target concentrations were rapidly equilibrating, then this model would reduce to a standard drug-binding model and SoA compartment would be unnecessary from a model-fitting perspective. For diseases such as RA and Crohn's disease, in which target concentrations are much higher in SoA than blood/plasma,[29,30] the current model structure represents a parsimonious approach to describe such physiological complexities. Model structure can also be modified to include membrane-bound targets, wherein target and complex distribution could initially be ignored. If targets are expressed on cells that distribute to other compartment (e.g., lymphocytes), then the model proposed here would be appropriate. A relevant starting assumption for the model with a membrane-bound target would be that drug-target complex in both plasma and SoA is eliminated at a rate

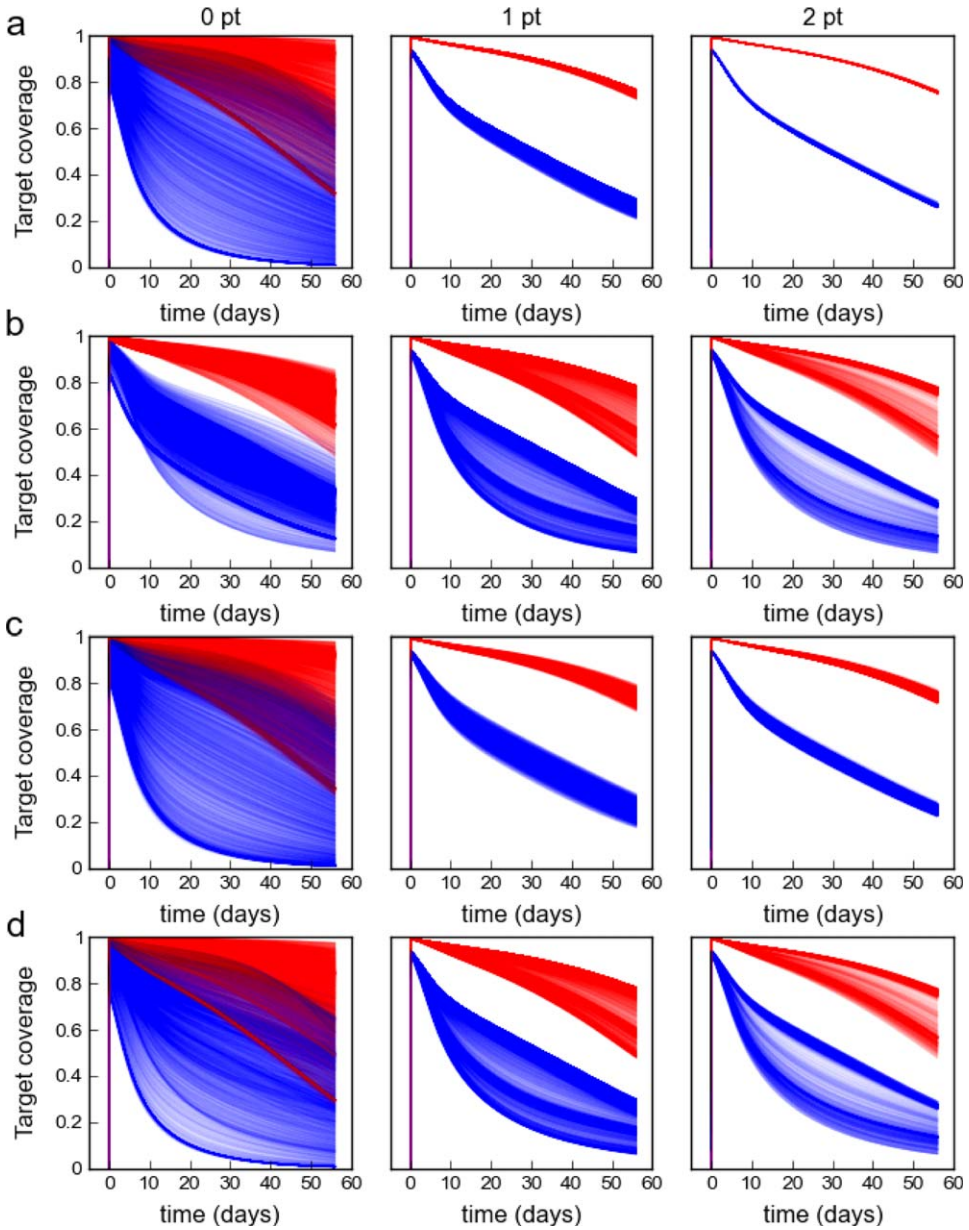

Figure 4 Effect of fixing a parameter on uncertainty in target coverage predictions. Target coverage predictions for case 1 in **Table 1** with fixed K_D (**a**), $Ratio_T$ (**b**), *thalfTp* (**c**), and T_{P0} (**d**) for 1 mg/kg (blue) and 10 mg/kg (red) i.v. dosing. Left, middle, and right panels are predictions for 0, 1, or 2 T_S^{tot} data points.

similar to free target. This assumption is rooted in the knowledge that many membrane-bound targets are internalized and drug binding does not hinder internalization. However, mechanism-based modeling of membrane-bound targets has shown that complex could be eliminated at a rate faster than free target.[34] The true elimination rate of complex would have to be determined through a model-fitting process. For the SoA model, complex elimination in tissue could impact drug PK and, in turn, be important to determine experimentally.

Pragmatically, a certain degree of uncertainty with model predictions is inevitable and therefore here an initial cutoff of 5% coverage uncertainty was considered acceptable in early development. However, significant uncertainty was observed in tissue-level predictions in absence of tissue data. When baseline target data in tissue was excluded during fitting, at least 50% of 32 datasets resulted in highly uncertain (>10%) coverage predictions (**Table 2**). An unexpected finding was that inclusion of baseline target data addressed this uncertainty inadequately (i.e., 13/32 datasets still had highly uncertain coverage predictions). These datasets were associated with slow protein turnover from at least one compartment. When both baseline and end-of-treatment tissue data were included, uncertainty in coverage predictions reduced significantly and a mere 3 of 32 datasets had moderate uncertainty (between 5 and 10%).

These observations suggest that when tissue data has not been characterized adequately one could wrongly predict target coverage for slow turnover targets.

Our analysis demonstrates that obtaining tissue biopsies and quantifying target levels can provide critical information on target coverage. Recently, baseline target levels in accessible tissues, like gut[35] and skin,[36] have been quantified. For soluble targets secreted from cells, accessible fraction is primarily localized to tissue interstitium with distribution to vascular space. This presents unique but surmountable challenges with regard to target quantification. For techniques like open-flow microperfusion,[3] drug and target measurements are primarily a direct read of interstitial fluid concentrations, whereas for tissue biopsy samples they are measured in total tissue. For drugs and targets that primarily reside in interstitial space, concentrations obtained from total tissue should be corrected for biopsy weight and interstitial volume, which is approximately one-third to one-tenth for most tissues.[4] If baseline and total target samples need to be assessed using different assays due to lower limit of quantification and/or drug interference limitations, then diligence in bridging both assays could help mitigate issues related to assay differences. Potentially one could conduct target spike-in experiments (drug naïve) *in vitro* such that levels are above the theoretical lower limit of quantification of both assays, and then determine whether the two assays can be bridged quantitatively. This bridge would allow for inferring free target baseline concentrations that would be consistent with total target assay. On the other hand, membrane-bound targets, not included in this work, are generally reported on a "number/cell" basis, which can be combined with Avogadro's number (6.023×10^{-23} mol^{-1}) and number of target-expressing cells within tissue to calculate an effective target concentration available in tissue interstitium for mAb binding. Unlike soluble targets, mAb binding to membrane-bound targets does not cause an increase in total target concentrations. Therefore, an mAb with a long PK half-life does not reduce complex elimination significantly relative to free target. In such cases, unless cell occupancy can be confirmed in an accessible compartment (e.g., peripheral blood) and used as a surrogate for SoA coverage, baseline total target level may be the only measure available to confirm model predictions.

In many cases, obtaining multiple tissue biopsies may be impossible due to physiological, technical, or ethical limitations. In such cases, an SoA model may be used to prospectively guide feasibility of achieving the required target coverage. Thus, we explored additional strategies that could reduce uncertainty in coverage predictions. GSA identified model parameters that significantly impact uncertainty in coverage predictions (**Figure 3**); thereby suggesting that fixing certain parameters could reduce uncertainty. Results from GSA can be method-dependent[25] and, therefore, to increase confidence in our analysis we used two established but different methods. Methods applied here should be viewed as orthogonal approaches that guide next steps toward fixing certain model parameters. Moreover, GSA does not take into account experimental feasibility of obtaining a parameter. For example, it showed coverage predictions are sensitive to target turnover rates. Methods exist for estimating protein turnover in tissues,[37] however, these are resource-intensive and require dosing of stable isotope labeled amino acid and assessing its incorporation into tissue proteins. By contrast, obtaining a plasma target turnover rate is easier and for known targets the rate constants can often be extracted from literature.[38–40] In some cases, clinical data on total target accumulation can be utilized to estimate both target and complex turnover rates.[41] In the absence of any information, *in vivo* studies with recombinant proteins in preclinical species may be used to estimate turnover rate, which can be allometrically scaled to humans.

Without an end-of-treatment tissue measurement, fixing *thalfTp* coupled with dose-ranging information (1 and 10 mg/kg; i.e., wide PK exposure) helped reduce uncertainty in coverage predictions (**Table 3**). Fixing T_{P0}, another sensitive parameter, had minimal impact on reducing uncertainty because we were already fitting T_{P0} within 7% error in our previous uncertainty analysis (**Table 2**). By definition, T_{P0} is the first data point for the time course of total target concentration in plasma. Similarly, fixing $Ratio_T$ (T_{S0}/T_{P0}) will have minimal impact, as we already constrain it by simultaneously fitting the time course of the total target concentration in plasma and baseline target concentration in tissue (1 tissue data point case). In a subset of scenarios (cases 24, 26, 28, 30, and 32), fixing either parameter, *thalf Tp* or T_{P0}, did not reduce uncertainty. All these cases share common features: mAb affinity to target is poor, target concentration (T_{P0} and T_{S0}) $\ll K_D$, and one of the target turnover rates is relatively slow (*thalfTs* or *thalfTp* = 24 h). We did not conduct a detailed analysis of this parameter space, however, if one encounters such a system in which affinity optimization is a challenge, then an end-of-treatment tissue biopsy or a dose-ranging study providing a wide range of PK exposures could be critical to inform tissue target coverage.

In conclusion, we have shown that the SoA model is useful for predicting target coverage in tissues in the presence of necessary data and model parameters. In the absence of biomarkers, this information is critical for ensuring the mechanism has been engaged adequately and subsequently guiding clinical decisions. Our analysis also elucidates basic tissue data requirements for successfully implementing such a model for target coverage predictions. Finally, alternative approaches for reducing coverage uncertainty were also explored to account for scenarios in which target measurement in tissues is impossible. However, it is recommended that a serious effort should be made to understand baseline levels of target in the relevant disease population.

Acknowledgments. We thank Hugh Barton for critically reviewing the manuscript and providing helpful suggestions to improve it.

Conflict of Interest. This study was sponsored by Pfizer. A.T., X.C., P.S., I.B., and H.M.J. are employees of Pfizer. A.Z. and A.K.A. were employees of Pfizer at the time of the study. Currently, A.Z. is at EMD Serono and A.K.A. is at Merck & Co., Inc.

Author Contributions. A.T. and A.A. wrote the manuscript. A.T., X.C., P.S., I.B., H.M.J., A.Z., and A.A. designed the research. A.T., H.L., P.J., and J.T. performed the research. A.T., H.L., X.C., P.S., I.B., P.J., J.T., H.M.J., A.Z., and A.A. analyzed the data. A.T., H.L., P.J., and J.T. contributed new reagents/analytical tools.

1. Leader, B., Baca, Q.J. & Golan, D.E. Protein therapeutics: a summary and pharmacological classification. *Nat. Rev. Drug Discov.* **7**, 21–39 (2008).
2. Smith, A.J. New horizons in therapeutic antibody discovery: opportunities and challenges versus small-molecule therapeutics. *J. Biomol. Screen.* **20**, 437–453 (2015).
3. Dragatin, C. *et al.* Secukinumab distributes into dermal interstitial fluid of psoriasis patients as demonstrated by open flow microperfusion. *Exp. Dermatol.* **25**, 157–159 (2016).
4. Baxter, L.T., Zhu, H., Mackensen, D.G., Butler, W.F. & Jain, R.K. Biodistribution of monoclonal antibodies: scale-up from mouse to human using a physiologically based pharmacokinetic model. *Cancer Res.* **55**, 4611–4622 (1995).
5. Miller, R. *et al.* How modeling and simulation have enhanced decision making in new drug development. *J. Pharmacokinet. Pharmacodyn.* **32**, 185–197 (2005).
6. Mager, D.E. & Jusko, W.J. General pharmacokinetic model for drugs exhibiting target-mediated drug disposition. *J. Pharmacokinet. Pharmacodyn.* **28**, 507–532 (2001).
7. Mager, D.E. & Krzyzanski, W. Quasi-equilibrium pharmacokinetic model for drugs exhibiting target-mediated drug disposition. *Pharm. Res.* **22**, 1589–1596 (2005).
8. Gibiansky, L. & Gibiansky, E. Target-mediated drug disposition model: approximations, identifiability of model parameters and applications to the population pharmacokinetic-pharmacodynamic modeling of biologics. *Expert Opin. Drug Metab. Toxicol.* **5**, 803–812 (2009).
9. Gibiansky, L., Gibiansky, E., Kakkar, T. & Ma, P. Approximations of the target-mediated drug disposition model and identifiability of model parameters. *J. Pharmacokinet. Pharmacodyn.* **35**, 573–591 (2008).
10. Jones, H. & Rowland-Yeo, K. Basic concepts in physiologically based pharmacokinetic modeling in drug discovery and development. *CPT Pharmacometrics Syst. Pharmacol.* **2**, e63 (2013).
11. Jones, H.M., Mayawala, K. & Poulin, P. Dose selection based on physiologically based pharmacokinetic (PBPK) approaches. *AAPS J.* **15**, 377–387 (2013).
12. Shah, D.K. & Betts, A.M. Towards a platform PBPK model to characterize the plasma and tissue disposition of monoclonal antibodies in preclinical species and human. *J. Pharmacokinet. Pharmacodyn.* **39**, 67–86 (2012).
13. Lachmann, H.J. *et al.* In vivo regulation of interleukin 1beta in patients with cryopyrin-associated periodic syndromes. *J. Exp. Med.* **206**, 1029–1036 (2009).
14. Chudasama, V.L., Zutshi, A., Singh, P., Abraham, A.K., Mager, D.E. & Harrold, J.M. Simulations of site-specific target-mediated pharmacokinetic models for guiding the development of bispecific antibodies. *J. Pharmacokinet. Pharmacodyn.* **42**, 1–18 (2015).
15. Cao, Y., Balthasar, J.P. & Jusko, W.J. Second-generation minimal physiologically-based pharmacokinetic model for monoclonal antibodies. *J. Pharmacokinet. Pharmacodyn.* **40**, 597–607 (2013).
16. Li, L., Gardner, I., Rose, R. & Jamei, M. Incorporating target shedding into a minimal PBPK-TMDD model for monoclonal antibodies. *CPT Pharmacometrics Syst. Pharmacol.* **3**, e96 (2014).
17. Weinblatt, M.E. *et al.* Adalimumab, a fully human anti-tumor necrosis factor alpha monoclonal antibody, for the treatment of rheumatoid arthritis in patients taking concomitant methotrexate: the ARMADA trial. *Arthritis Rheum.* **48**, 35–45 (2003).
18. Maini, R. *et al.* Infliximab (chimeric anti-tumour necrosis factor alpha monoclonal antibody) versus placebo in rheumatoid arthritis patients receiving concomitant methotrexate: a randomised phase III trial. ATTRACT Study Group. *Lancet* **354**, 1932–1939 (1999).
19. Stepensky, D. Local versus systemic anti-tumour necrosis factor-α effects of adalimumab in rheumatoid arthritis: pharmacokinetic modelling analysis of interaction between a soluble target and a drug. *Clin. Pharmacokinet.* **51**, 443–455 (2012).
20. Brodfuehrer, J. *et al.* Quantitative analysis of target coverage and germinal center response by a CXCL13 neutralizing antibody in a T-dependent mouse immunization model. *Pharm. Res.* **31**, 635–648 (2014).
21. Foote, J. & Eisen, H.N. Breaking the affinity ceiling for antibodies and T cell receptors. *Proc. Natl. Acad. Sci. USA* **97**, 10679–10681 (2000).
22. Singh, P., Tiwari, A., Abraham, A.K. & Zutshi, A. Application of mechanistic pharmacokinetic–pharmacodynamic modeling toward the development of biologics. In *Developability of Biotherapeutics: Computational Approaches* (eds. Kumar, S. & Singh, S.K.) 109–134 (CRC Press, Boca Raton, FL, 2015).
23. Dirks, N.L. & Meibohm, B. Population pharmacokinetics of therapeutic monoclonal antibodies. *Clin. Pharmacokinet.* **49**, 633–659 (2010).
24. Goh, C.J. & Keo, K.L. Control parametrization: a unified approach to optimal control problems with general constraints. *Automatica (Oxf)* **24**, 3–18 (1988).
25. Marino, S., Hogue, I.B., Ray, C.J. & Kirschner, D.E. A methodology for performing global uncertainty and sensitivity analysis in systems biology. *J. Theor. Biol.* **254**, 178–196 (2008).
26. Kim, K.A. *et al.* Systematic calibration of a cell signaling network model. *BMC Bioinformatics* **11**, 202 (2010).
27. Gutenkunst, R.N., Waterfall, J.J., Casey, F.P., Brown, K.S., Myers, C.R. & Sethna, J.P. Universally sloppy parameter sensitivities in systems biology models. *PLoS Comput. Biol.* **3**, 1871–1878 (2007).
28. Kuester, K. & Kloft, C. Chapter 3. Pharmacokinetics of monoclonal antibodies. In *Pharmacokinetics and Pharmacodynamics of Biotech Drugs: Principles and Case Studies in Drug Development* (ed. Meibohm, B.). (Wiley, Hoboken, NJ, 2006).
29. Partsch, G., Steiner, G., Leeb, B.F., Dunky, A., Bröll, H. & Smolen, J.S. Highly increased levels of tumor necrosis factor-alpha and other proinflammatory cytokines in psoriatic arthritis synovial fluid. *J. Rheumatol.* **24**, 518–523 (1997).
30. McInnes, I.B. & Schett, G. Cytokines in the pathogenesis of rheumatoid arthritis. *Nat. Rev. Immunol.* **7**, 429–442 (2007).
31. Gearing, A.J. *et al.* Cytokines in skin lesions of psoriasis. *Cytokine* **2**, 68–75 (1990).
32. Papadakis, K.A. & Targan, S.R. Role of cytokines in the pathogenesis of inflammatory bowel disease. *Annu. Rev. Med.* **51**, 289–298 (2000).
33. Kelso, A. Cytokines: principles and prospects. *Immunol. Cell Biol.* **76**, 300–317 (1998).
34. Jager, E., van der Velden, V.H., te Marvelde, J.G., Walter, R.B., Agur, Z. & Vainstein, V. Targeted drug delivery by gemtuzumab ozogamicin: mechanism-based mathematical model for treatment strategy improvement and therapy individualization. *PLoS One* **6**, e24265 (2011).
35. Palandra, J., Finelli, A., Zhu, M., Masferrer, J. & Neubert, H. Highly specific and sensitive measurements of human and monkey interleukin 21 using sequential protein and tryptic peptide immunoaffinity LC-MS/MS. *Anal. Chem.* **85**, 5522–5529 (2013).
36. Neubert, H. *et al.* Tissue bioanalysis of biotherapeutics and drug targets to support PK/PD. *Bioanalysis* **4**, 2589–2604 (2012).
37. Garlick, P.J., McNurlan, M.A., Essén, P. & Wernerman, J. Measurement of tissue protein synthesis rates in vivo: a critical analysis of contrasting methods. *Am. J. Physiol.* **266**(3 Pt 1), E287–E297 (1994).
38. Hovgaard, D., Mortensen, B.T., Schifter, S. & Nissen, N.I. Comparative pharmacokinetics of single-dose administration of mammalian and bacterially-derived recombinant human granulocyte-macrophage colony-stimulating factor. *Eur. J. Haematol.* **50**, 32–36 (1993).
39. Saks, S. & Rosenblum, M. Recombinant human TNF-alpha: preclinical studies and results from early clinical trials. *Immunol. Ser.* **56**, 567–587 (1992).
40. Kurzrock, R. *et al.* Pharmacokinetics, single-dose tolerance, and biological activity of recombinant gamma-interferon in cancer patients. *Cancer Res.* **45**, 2866–2872 (1985).
41. Tiwari, A., Kasaian, M., Heatherington, A.C., Jones, H.M. & Hua, F. A mechanistic PK/PD model for two anti-IL13 antibodies explains the difference in total IL-13 accumulation observed in clinical studies. *MAbs* **8**, 983–990 (2016).

Supplementary information accompanies this paper on the *CPT: Pharmacometrics & Systems Pharmacology* website (http://www.wileyonlinelibrary.com/psp4)